





## Special Issue Research Article

# Photodynamic Activity on Biofilm in Endotracheal Tubes of Patients Admitted to an Intensive Care Unit<sup>†</sup>

Rosane Bassi Soares<sup>1</sup>, Denis Honorato Costa<sup>1</sup>, Walter Miyakawa<sup>2</sup>, Maria Goretti Temoteo Delgado<sup>3</sup>, Aguinaldo Silva Garcez<sup>3</sup>, Tania Mateus Yoshimura<sup>4</sup>, Martha Simões Ribeiro<sup>4</sup>  and Silvia Cristina Nunez<sup>1\*</sup> 

<sup>1</sup>Post Graduation Program Biomedical Engineering and Bioengineering, Universidade Brasil, Sao Paulo, Brazil

<sup>2</sup>Instituto de Estudos Avançados, Sao Jose dos Campos, Brazil

<sup>3</sup>São Leopoldo Mandic Dental Research Center, Campinas, Brazil

<sup>4</sup>Nuclear and Energy Research Institute, IPEN/CNEN-SP, São Paulo, Brazil

Received 14 October 2019, accepted 7 January 2020, DOI: 10.1111/php.13239

## ABSTRACT

Ventilator-associated pneumonia (VAP) is an infection that arises after endotracheal intubation affecting patients under intensive care. The presence of the endotracheal tube (ETT) is a risk factor since it is colonized by multispecies biofilm. Antimicrobial photodynamic therapy (aPDT) could be a strategy to decontaminate ETTs. We verify if methylene blue (MB) associated with external illumination of the ETT could be an alternative to destroy biofilm. We performed an *in vitro* and *ex vivo* study. *In vitro* study was performed with *P. aeruginosa* biofilm grew over ETT for 7 days. After treatment, the surviving cells were cultured for 3 days and the biofilm was analyzed by crystal violet absorbance. *Ex vivo* study employed ETT obtained from extubated patients. aPDT was performed with MB (100  $\mu$ M) and red LED ( $\lambda = 640 \pm 20$  nm). We quantified the biofilm thickness and used scanning electron microscopy and fluorescence technique to verify morphological and functional changes after aPDT. Our results showed that bacteria remain susceptible to aPDT after sequential treatments. We also attested that aPDT can reduce biofilm thickness, disrupt biofilm attachment from ETT surface and kill microbial cells. These data suggest that aPDT should be investigated to decrease VAP incidence via ETT decontamination.

## INTRODUCTION

The photodynamic effect has been studied for more than a century and it presents multiple applications ranging from environmental microbial control to cancer treatment. Everyone that starts to study photodynamic therapy (PDT) read or hear about some researchers that could be considered the “founding fathers” of PDT applications and principles. The initial researchers are Hermann von Tappeiner and Oscar Raab that were the

first researchers to describe the photodynamic effect. The second researcher is Lipson with the proof of concept that PDT could be a clinical application. The third, and most likely, the one that brought more attention and visibility to the therapy is Prof. Dougherty and the work developed by his group at the Roswell Park Cancer Institute. Prof. Dougherty's work in the 70s of past century was recognized worldwide, and several research centers all over the world followed his steps and introduced PDT as a cancer therapy among their investigation interests.

Besides the direct contribution to clinical PDT advances, Prof. Dougherty went beyond and found a research foundation to support new students and advances in the field. It is not exaggerated to state that everyone that is nowadays studying all types of PDT applications owe somehow to Prof. Dougherty a recognition for his life and work.

Besides cancer treatment, PDT also grows as an antimicrobial therapy. The same principles and mechanisms of action are applied with different targets. Microbial cells present different sensitivities to the oxidative stress promoted by the photodynamic action but, in general, there is no selection of resistant microorganisms to antimicrobial PDT (aPDT) (1). Microorganisms may evolve from planktonic cells to a well-organized system attached to a surface known as biofilm. Biofilms are biological communities with a high degree of organization, where microbial cells form structured, coordinated and functional communities. These biological communities are embedded in polymeric matrixes produced by the cells becoming most of the time recalcitrant to antimicrobial treatment. Microbial biofilms are responsible for most of the infections in humans (2), and aPDT has been successfully used to treat different biofilm-related infections (3-6).

Critically ill patients receiving mechanical ventilation are at risk of developing ventilator-associated pneumonia (VAP), which is considered a healthcare-related infection with high incidence in intensive care units (ICUs), being responsible for high morbidity and mortality rates (7). In fact, VAP is held responsible for an estimated 29% of all deceases in intensive care units with even higher percentages being described (8). Prevention of VAP

\*Corresponding author email: silvianunez@uol.com.br (Silvia Cristina Nunez)

<sup>†</sup>This article is part of a Special Issue dedicated to Dr. Thomas Dougherty.

© 2020 American Society for Photobiology

appears to have a major potential to reduce ICU mortality, and it can also reduce antibiotic use, which is an important issue in the context of antimicrobial drug resistance, since it is estimated that approximately 50% of total antibiotic use in ICUs is for treating VAP (9).

The presence of an endotracheal tube (ETT), which is an essential part of the mechanical ventilation system, results in a break of the host natural defense mechanisms and facilitates pathogen inoculation of the lower respiratory tract. The ETT and the mechanical ventilation can contribute to the risk of VAP in several ways, as for instance, aspiration during intubation or subsequently, presence of secretions around the ETT cuff, biofilm in the ETT, impairment of mucociliary function, secretions from other areas as sinuses or oropharynx, and positive pressure from the ventilator (10).

Antimicrobials have long been the only way to fight infection, and several bacteria, mostly in ICU, have become resistant to the indiscriminate use of antibiotics (11). Thus, the aPDT could be an innovative and effective alternative as a defensive measure against VAP. In fact, Biel et al. showed that methylene blue (MB)-mediated aPDT can effectively inactivate *Pseudomonas aeruginosa* and methicillin-resistant *Staphylococcus aureus* biofilms formed inside an ETT after a single application, using an internal light source, placed inside the ETT (12). To place an optical fiber inside the ETT requires differentiated biomedical instrumentation. However, the authors purposed the insertion of an optical diffuser fiber connected to a light source and the tubes would be illuminated by the inside area.

Our study was designed to evaluate the effect of an external light source reaching the ETT from the outer layer. To evaluate the aPDT performance with an external light source, we first grew biofilms of *P. aeruginosa* on ETT, applied aPDT using MB and a red laser, and confirmed aPDT efficacy. Later, we grew a new biofilm with surviving bacteria to verify whether bacteria were still susceptible to oxidative stress caused by the same aPDT parameters. As most biofilm studies analyze mono- or duo-species cultures, whereas nearly all biofilm in nature contains a diversity of microorganisms, we posteriorly evaluated aPDT on real ETT biofilms obtained from extubated patients that were hospitalized in ICU with more than 4 days of use, using a LED system and MB to perform aPDT. This represents a multiple species biofilm; therefore, it would be closer to the real challenge in an ICU situation.

## MATERIALS AND METHODS

*Pseudomonas aeruginosa* biofilm growth. *Pseudomonas aeruginosa* ATCC 9027 was firstly used since it is commonly involved in VAP (13). Bacterial cells were maintained through subculturing on brain–heart infusion (BHI; Difco, USA). Culture was aerobically grown in BHI broth at 37°C for 24 h. Test tubes with 500  $\mu$ L BHI were contaminated with 500  $\mu$ L of *P. aeruginosa* in suspension and incubated at 37°C for 24 h, giving a final cell concentration of  $4 \times 10^7$  CFU mL<sup>-1</sup>.

To grow the biofilm, sterilized samples of ETT measuring  $1 \times 1$  cm were previously prepared and then they were submerged into a Petri dish containing 20 mL of BHI broth contaminated with 1 mL of the bacterial suspension for 7 days at 37°C. The BHI broth was replaced every 24 h, allowing the formation of biofilm. The samples were then rinsed with saline solution to remove nonadherent cells from the biofilm and randomly divided into control and aPDT groups. The samples from control group ( $n = 15$ ) did not receive any treatment. The samples were rinsed again with 10 mL of saline solution to simulate a bronchoalveolar lavage. The samples from aPDT group ( $n = 15$ ) received with a syringe a water solution of 500  $\mu$ L of MB at 100  $\mu$ M that was kept in the dark for 1 min and then irradiated with a diode laser ( $\lambda = 660$  nm, P = 100 mW; Laser Duo

MMOptics, Brazil) receiving a total of 6 J of energy. Three sets of independent experiments were performed.

After each experiment, the samples were placed inside a sterile 1.5 mL microcentrifuge tube, which was subsequently sealed and vortexed for 1 min. They were then challenged with low-output ultrasonication to unbind the biofilm. One hundred  $\mu$ L aliquots were added to the wells of a 96-well plate for serial dilution and streaking on square BHI agar plates. The plates were incubated using standard aerobic conditions at 37°C for 24 h for colony-forming unit (CFU) counting.

The bacteria that survive from aPDT were then incubated in a 96-well plate for 72 h as described above. After biofilm growth, the wells were washed with saline solution to remove nonadherent cells from the biofilm and stained with 1% solution of crystal violet (100  $\mu$ L each well) for 15 min. Thereafter, they were washed three times with PBS and dried at room temperature. The absorbance of adherent biofilm cells was measured with a microplate reader (Epoch, BioTek, USA) at  $\lambda = 570$  nm. The measurements were performed each 24 h during three consecutive days.

*Biofilm from extubated patients.* The samples analyzed were obtained from ETTs removed from patients admitted to the ICU of Hospital São Francisco de Assis (São Paulo, Brazil), who remained for more than 96 h under mechanical ventilation, with clinical suspicion of VAP. This study was approved by the Ethics Committee (CAAE 66492217.5.00005494), and the patient or his/her legal representative signed the informed consent form. We performed images of the inside part of the tubes to confirm the biofilm structure and its characteristic.

For the photodynamic inactivation, ETTs with more than 4 days of use in patients under mechanical ventilation were included. Immediately after extubation, they were cut with a scalpel blade 6 cm distally. Each ETT was placed in a sterile vial with 50 mL of 0.9% saline solution. Posteriorly, they were washed with 30 mL of 0.9% saline solution and cut into three fragments of  $2 \times 2$  cm. One fragment was washed again with 15 mL of 0.9% saline and transferred to a sterile vial with 20 mL of 2% glutaraldehyde for 24 h for fixation of the biofilm. This fragment was considered control for this specific tube. Another fragment was covered with 5 mL of MB (Sigma Aldrich, USA) solution at a concentration of 100  $\mu$ M diluted in distilled water applied with a syringe on the inside part of the tube. The sample remained covered with aluminum foil for 5 min in a dark environment. It was then washed with 15 mL of 0.9% saline and transferred to a sterile vial containing 20 mL of glutaraldehyde with 2% for biofilm fixation. This fragment was considered photosensitizer control for the respective tube. The third fragment received the MB solution as described above and remained for 5 min covered with aluminum foil. Afterward, photodynamic inactivation was performed with a red LED ( $\lambda = 640 \pm 20$  nm) on the external part of the tube without any biofilm disruption. The light parameters were 100 mW for 10 min delivering 60 J divided into two irradiations with 5 min each with 1 min of dark between irradiations. All images were observed under light microscopy and by scanning electron microscopy (SEM) (TabletopMicroscope, TM 3000 Hitachi, Japan).

To measure the biofilm thickness immediately after extubation, ETTs were cut and washed as previously described and they were placed in a Falcon tube containing 15 mL of BHI culture medium and sent for refrigeration, until SEM imaging. External marks were performed on the tubes to delimit the area to be observed. After imaging and measurement, photodynamic inactivation was performed in each section according to the proposed parameters. At the end of the photodynamic inactivation, the samples were washed with 15 mL of saline solution and each fragment was placed in a sterile vial to be analyzed by SEM. The biofilm thickness was measured in 10 distinct locations along the ETT as shown in Fig. 1.

Microbial viability was measured through fluorescence analysis using BacLight LIVE/DEAD viability kit (Molecular Probe, USA). In the kit, there are two fluorescent nucleic acids: SYTO9 (green fluorescence) that identifies viable bacteria and propidium iodide (PI; red fluorescence) that identifies nonviable bacteria. To assess viability, one- $\mu$ L of solution was added to 3 mL of sterile saline (0.9%). Over the sample, 70  $\mu$ L of the solution was dispensed and then incubated for 15 min in the dark at room temperature. Biofilm samples were examined under a fluorescence microscope (Zeiss, Germany) using oil immersion objective (100 $\times$ ). The excitation wavelength was 488 nm and 525 nm for SYTO9 and PI, respectively. Posteriorly, color channels were split into green, red and blue using ImageJ. The areas of green and red were threshold-adjusted to highlight the living and dead cells and subtract the background fluorescence signal. The integrated densities of the threshold areas were

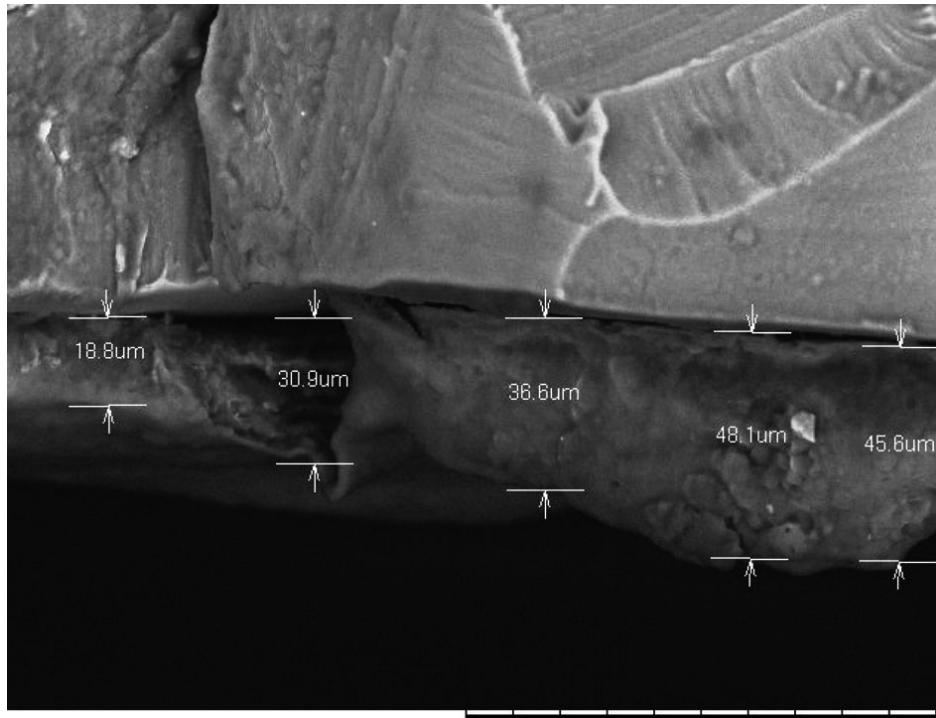


**Figure 1.** The SEM micrograph of multispecies biofilms in ETTs of extubated patients illustrating as the biofilm thickness was quantified. Bars represent 100  $\mu\text{m}$ .

obtained for each channel, and the intensity ratio of green over red was calculated.

## RESULTS

In our first assay, the number of viable cells of the control group did not vary even after irrigation with 100 mL of saline solution. After aPDT, a complete eradication was not observed as expected. In fact, there was a reduction of approximately 5 logs compared to control group and, at least, 2 logs of bacteria still survive following aPDT. The initial count was approximately  $5 \times 10^8 \text{ CFU mL}^{-1}$  and the final results demonstrated a mean of  $7 \times 10^3 \text{ CFU mL}^{-1}$ .

Regarding biofilm formed by surviving cells, our data show that bacteria were also susceptible to aPDT. In fact, we can observe that biofilm formation was significantly affected (Fig. 2). Interestingly, it seems that bacteria slow down their growth in the first 24 h since biofilm of control group formed 3-fold more biomass than aPDT group. However, following 48 h and 72 h, the quantity of biofilm was about 2-fold higher for control compared to aPDT group.

Images of ETTs from patients that underwent mechanical ventilation are presented in Fig. 3. ETTs were uniformly covered with biofilm. The extension and morphology of biofilm was variable according to the days of use by the patient. We observed some ETTs with scarce (Fig. 3a,b) or abundant biofilm matrices as shown in Fig. 3c. We also identified different microorganisms immersed in the biofilm matrix as cocci, bacilli and yeasts.

In a panoramic view, without aPDT, we can observe an abundant biofilm with complex matrices in the inner surface of the ETTs (Fig. 4a). After aPDT, the ETT surface changed dramatically. We noticed compaction of the biofilm matrix rendering the ETT wall visible. Microorganisms were not perceptible (Fig. 4b).

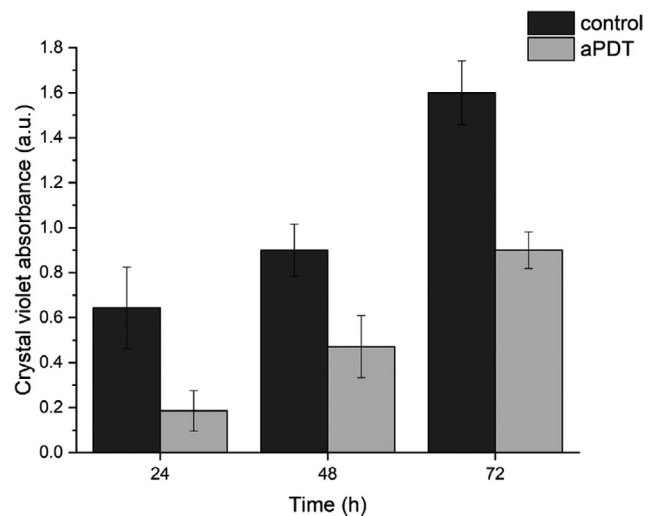


**Figure 2.** Means  $\pm$  standard deviation of the absorbance at  $\lambda = 570 \text{ nm}$  of crystal violet that is correlated to the biofilm biomass. Observe that surviving bacterial cells are still susceptible to aPDT. In addition, biomass increases over time. A set of three independent experiments were performed.

In fact, Fig. 5 depicts the biofilm detachment from the ETT surface following aPDT in a higher magnification. Of note, these results were obtained only 10 min after illumination with 100  $\mu\text{m}$  of MB.

Figure 6 presents the mean thickness of biofilms formed in eight different ETTs. Regardless the days of use by the patient, the biofilm thickness decreased in all samples. These results

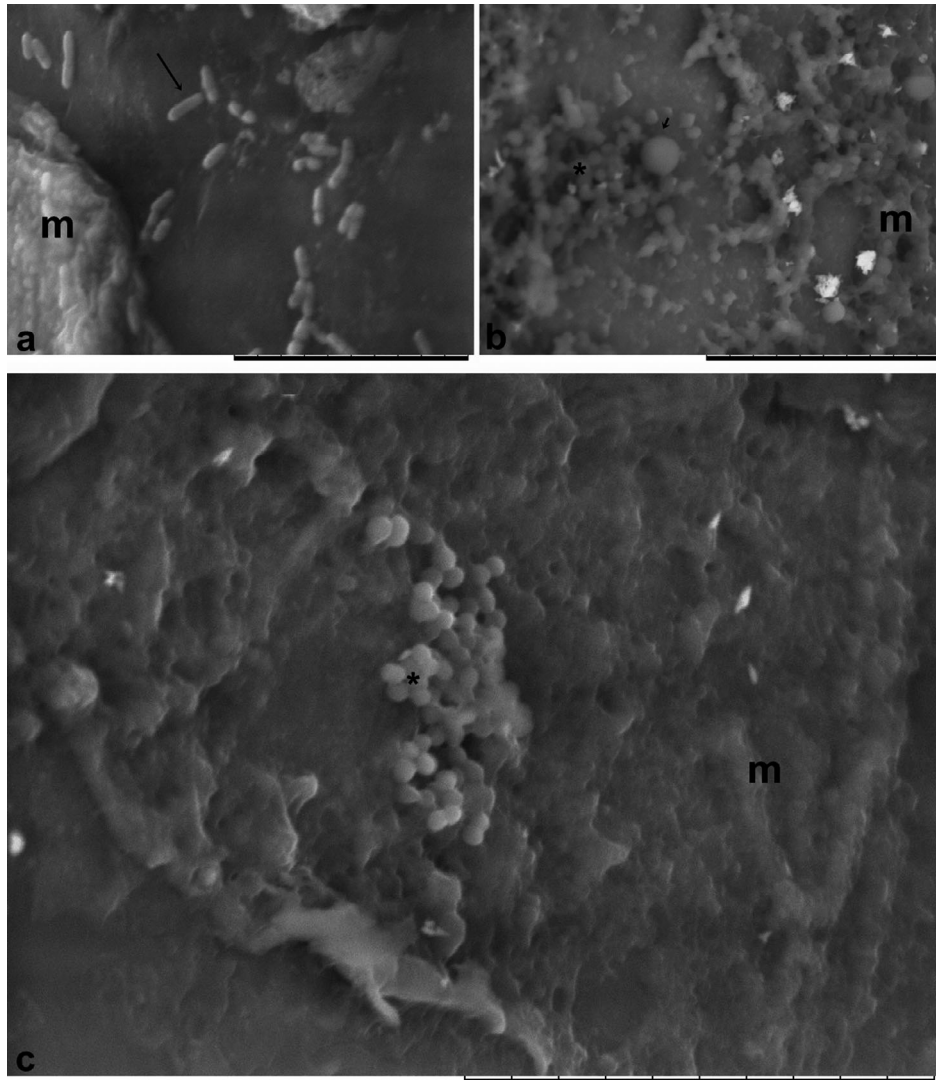


**Figure 3.** The SEM micrographs of multispecies biofilms in ETTs of extubated patients after 7 days (a), 8 days (b) and 14 days of use. Bacilli (arrow), yeast (arrowhead) and cocci (\*) can be noticed. Observe scarce (a, b) and dense (c) matrices that are attached on the surface of the ETT (m). Bars represent 10  $\mu\text{m}$  (a) and 20  $\mu\text{m}$  (b, c).

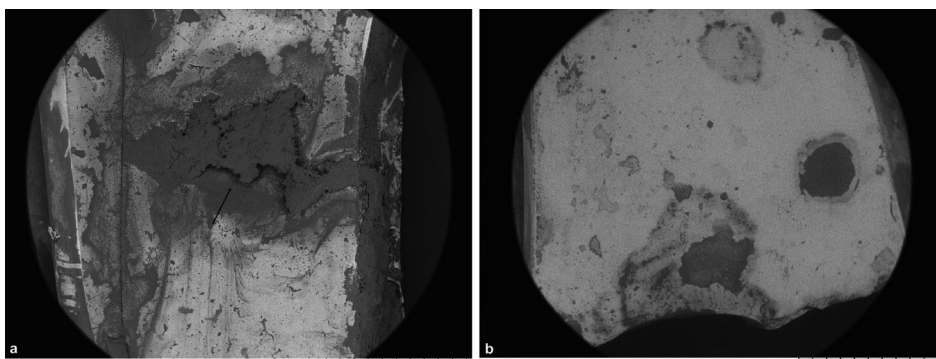


**Figure 4.** The SEM micrographs of multispecies biofilms in ETTs of extubated patients after 13 days of use before (a) and after aPDT (b). Observe the degradation of the biofilm structure after aPDT. Bars represent 2 mm.

demonstrate the action of aPDT and its property to condense and degrade the biofilm matrix that further may uncover the microorganisms rendering them more susceptible to antimicrobial agents and increasing the ETT lumen.

Figure 7 exhibits fluorescence images obtained with dead/alive fluorescence probes. Before aPDT, we observed the green emission characteristic of live cells (Fig. 7a). In contrast, the red emission denotes that aPDT was able to inactivate

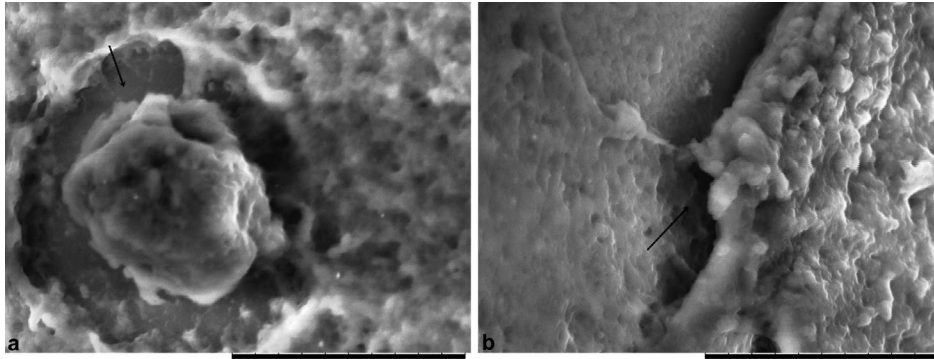


**Figure 5.** The SEM micrographs of multispecies biofilms in ETTs of extubated patients after 13 days of use following fractionated aPDT in a frontal (a) and lateral view (b). The arrows point to the detachment of the biofilm from ETT surface.

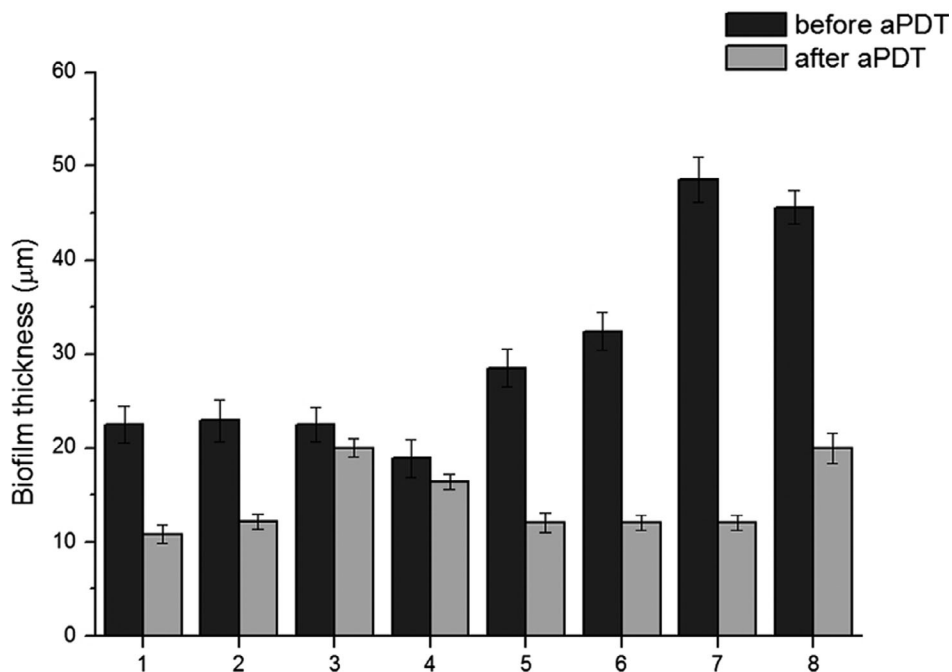


**Figure 6.** Mean values  $\pm$  standard deviation of the biofilm thickness before and after fractionated aPDT. Observe that the thickness decreases regardless the days of use of ETT by patients.

microbial cells (Fig. 7b). In fact, the green fluorescence is about 1.1-fold higher than red fluorescence before aPDT. After treatment, the rate of green and red fluorescence is around 0.3 (Fig. 7c).

## DISCUSSION

Our study showed, to the best of our knowledge, for the first time the effect of aPDT over biofilms obtained from ETT of extubated patients from an ICU, which represents a real challenge to all antimicrobial strategies. We verified that MB-mediated aPDT was able to reduce biofilm and to promote its detachment from ETT walls, regardless the time of biofilm growth.

Some studies have proposed to use aPDT to fight pneumonia using different approaches (12,14,15). Biel *et al.* showed that a dual species biofilm could be efficiently reduced inside the ETT applying aPDT (12). Their results were promising, and their protocol required the use of a system with the optical diffusor been

placed inside the ETT and, therefore, the use of a dedicated light source.

Meanwhile, a clinical trial registered and probably still being executed proposed the use of aPDT with MB as a mouthwash formulation and a red LED to reduce oral colonization in patients in ICU. The authors will try to elucidate the relationship between the decontamination and VAP incidence (14). In fact, to control oral colonization appears to be an important factor to prevent VAP (16).

Another study performed by Kassab *et al.* demonstrated the possibility of treating pneumonia with aPDT. They proposed an alternative approach with the use of a nebulization system to deliver the photosensitizer and the employment of an external light source to activate it (15). Based on the assumption that an external light source could be used, our group performed an investigation about light penetration inside ETT covered with biofilm and we demonstrated that light can be efficiently delivered from the outer part of the tube (17).

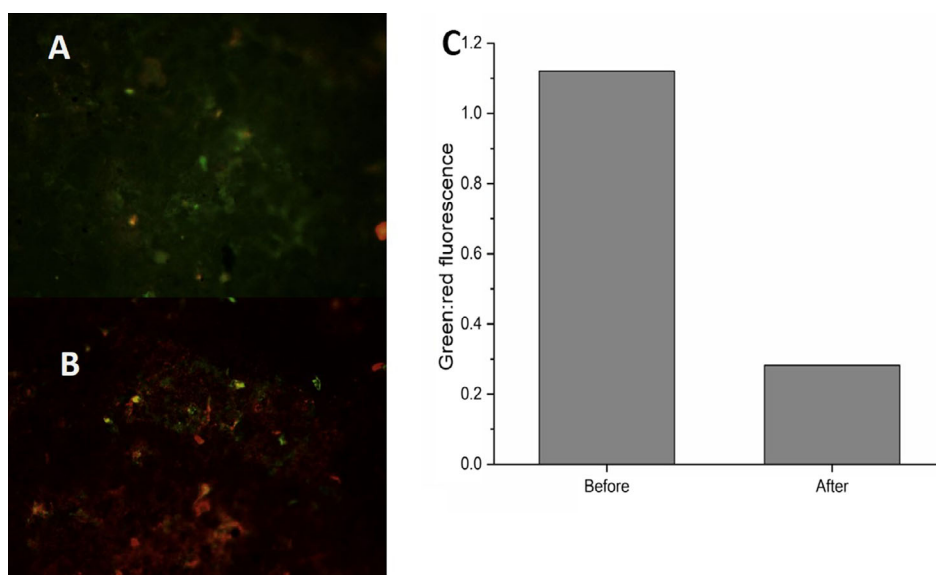


**Figure 7.** Fluorescence micrographs of multispecies biofilms in ETTs of extubated patients after 13 days of use before (a) and after aPDT (b) stained by live/dead kit. The rate of green (living cells) and red (dead cells) fluorescence drastically changes after aPDT (c).

In this study, our first step was to evaluate the external illumination over a *P. aeruginosa* biofilm since these bacteria are often involved in VAP (18). We observed a reduction in microbial viability which is in accordance with previous studies (19,20) but using illumination through the ETT.

Probably, in a real ICU environment, the ETT decontamination will have to be performed several times. Therefore, we decided to verify the susceptibility of the surviving cells and their capacity to form biofilms. In fact, these two features are important since susceptibility from the surviving cells means that aPDT could be repeated several times in a clinical setting. Regarding biomass, its presence is responsible for a worst diffusion of any antimicrobial agent. Our results showed that viable cells after aPDT could still be affected by the same light dose and photosensitizer concentration. In addition, less biomass was noticed.

Analyzing the growth rate on the surviving cells after aPDT, we observed at the beginning a slower growth compared with control cells but followed by a recover after 48 h. According to de Melo et al., cells that survive to aPDT may present an overexpression of genes that promote a slower growth rate for the persistent population (21). Consistent with our results, it may happen immediately after aPDT, probably due to a phenotype change of the cells, but the phenomenon could not be observed on the following growth analyses.

On the *ex vivo* ETT biofilm analyses, we opted to perform a microscopy study to preserve the natural architecture of the biofilm. Moreover, ETT contains multiple microorganisms and the most of them are considered unculturable (22). We observed the presence of different types of bacteria as rods, coccus and fungi on the images. Due to the nature of the sample, it is virtually impossible to obtain all samples with the same day of use, and even in that case, it would be not guaranteed that the same level of contamination would be encountered.

There is a wide variety of information about the timeline of biofilm formation on ETT and about type of colonization (22).

Besides that, the importance of ETT colonization for the development of VAP has long been recognized. In fact, Pneumatikos et al. recommended the change on VAP nomenclature to endotracheal tube-associated pneumonia (23). In our study, the criteria to select a given ETT from a patient was the medical diagnostic of VAP, this variable was selected to guarantee that our samples would be of clinical significance.

In a pilot study, we evaluated two types of irradiation: 10 min continuously or 10 min divided into times of 5 min since some studies report better results for fractionated doses when applying aPDT on monospecies biofilm (24,25). In fact, we observed a better result for fractionated light, mostly on the interface biofilm/tube wall. This result may be related to different reactive oxygen species formation and diffusion time, but these data require further investigation.

Biofilm detachment and dispersion of extracellular polymeric substance (EPS) of biofilm play an important role in our results. Although the dead/alive fluorescence microscopy showed that most of the cells at the image were affected by the oxidative stress, live cells certainly would be responsible for the recolonization of the tube. On the other hand, the detachment of the surface may indicate that would be easier to remove the biofilm with devices such as a mucus shaver (26), which would allow the maintenance of the tube lumen with appropriate ventilation and less accumulation of mucus and bacterial growth.

The EPS contains a variety of substances as polysaccharides, proteins, hexosamine and DNA, and it is the first line of defense against most threats, including aPDT (27). Moreover, the EPS limits inward diffusion of antimicrobial agents that can make the biofilm resistant. Our results showing the disruption of the matrix have already been observed in previous studies from our group in *P. aeruginosa* and *E. faecalis* biofilms after MB-mediated aPDT (28), and they can represent an important line of investigation to be pursued, mostly, concerning the employment of aPDT simultaneously with other antimicrobial

strategies. Furthermore, the importance of biofilm thickness is still under investigation in terms of community composition and ecosystem function (29).

In terms of VAP, our results showed that it is possible to diminish the EPS content, to kill microbial cells and to detach the biofilm from the ETT wall. Taking together, these results may represent an important step toward a new antimicrobial strategy to prevent VAP.

*Acknowledgements*—M.S. Ribeiro would like to thank the National Institute of Photonics (INFO, INCT/CNPq grant # 465763/2014-6) for financial support.

## REFERENCES

- Cieplik, F., D. Deng, W. Crielard, W. Buchalla, E. Hellwig, A. Al-Ahmad and T. Maisch (2018) Antimicrobial photodynamic therapy – what we know and what we don't. *Crit. Rev. Microbiol.* **44**, 571–589.
- Orazi, G. and G. A. O'Toole (2019) 'It takes a village': mechanisms underlying antimicrobial recalcitrance of polymicrobial biofilms. *J. Bacteriol.* **202**, e00530-19.
- Garcez, A. S., S. C. Nunez, M. R. Hamblin and M. S. Ribeiro (2008) Antimicrobial effects of photodynamic therapy on patients with necrotic pulps and periapical lesion. *J. Endod.* **34**, 138–142.
- Alvarenga, L. H., A. C. Gomes, P. Carribeiro, B. Godoy-Miranda, G. Noschese, M. Simoes Ribeiro, I. T. Kato, S. K. Bussadori, C. Pavani, Y. G. E. Geraldo, D. Silva, A. Horliana, M. Wainwright and R. A. Prates (2019) Parameters for antimicrobial photodynamic therapy on periodontal pocket-Randomized clinical trial. *Photodiagnosis Photodyn. Ther.* **27**, 132–136.
- Scwingel, A. R., A. R. Pinheiro Barcessat, S. C. Nunez and M. S. Ribeiro (2012) Antimicrobial photodynamic therapy in the treatment of oral candidiasis in HIV-infected patients. *Photomed. Laser Surg.* **30**, 429–432.
- Tardivo, J. P., M. Wainwright and M. Baptista (2015) Small scale trial of photodynamic treatment of onychomycosis in Sao Paulo. *J. Photochem. Photobiol. B* **150**, 66–68.
- Haque, M., M. Sartelli, J. McKimm and M. Abu Bakar (2018) Health care-associated infections – an overview. *Infect. Drug Resist.* **11**, 2321–2333.
- Zarb, P., B. Coignard, J. Griskeviciene, A. Muller, V. Vankerckhoven, K. Weist, M. m Goossens, S. Vaerenberg, S. Hopkins, B. Catry, D. I Monnet, H. Goossens, C. Suetens, and Collective Hospital Contact Points for the ECD (2012) The European Centre for Disease Prevention and Control (ECDC) pilot point prevalence survey of healthcare-associated infections and antimicrobial use. *Euro Surveill.* **17**, pii: 20316.
- Hunter, J. D. (2012) Ventilator associated pneumonia. *BMJ* **344**, e3325.
- Mehta, A. and R. Bhagat (2016) Preventing ventilator-associated infections. *Clin. Chest Med.* **37**, 683–692.
- Luyt, C. E., G. Hekimian, D. Koulenti and J. Chastre (2018) Microbial cause of ICU-acquired pneumonia: hospital-acquired pneumonia versus ventilator-associated pneumonia. *Curr. Opin. Crit. Care* **24**, 332–338.
- Biel, M. A., C. Sievert, M. Usacheva, M. Teichert, E. Wedell, N. Loebel, A. Rose and R. Zimmermann (2011) Reduction of endotracheal tube biofilms using antimicrobial photodynamic therapy. *Lasers Surg. Med.* **43**, 586–590.
- Fernandez-Barat, L., M. Ferrer, F. De Rosa, A. Gabarrus, M. Esperatti, S. Terraneo, M. Rinaudo, G. Li Bassi and A. Torres (2017) Intensive care unit-acquired pneumonia due to *Pseudomonas aeruginosa* with and without multidrug resistance. *J. Infect.* **74**, 142–152.
- Da Collina, G. A., A. C. R. Tempestini-Horliana, D. F. T. da Silva, P. L. Longo, M. L. F. Makabe and C. Pavani (2017) Oral hygiene in intensive care unit patients with photodynamic therapy: study protocol for randomised controlled trial. *Trials* **18**, 385.
- Kassab, G., M. C. Geralde, N. M. Inada, A. E. Achilles, V. G. Guerra and V. S. Bagnato (2019) Nebulization as a tool for photosensitizer delivery to the respiratory tract. *J. Biophotonics* **12**, e201800189.
- Pedreira, M. L., D. M. Kusahara, W. B. de Carvalho, S. C. Nunez and M. A. Peterlini (2009) Oral care interventions and oropharyngeal colonization in children receiving mechanical ventilation. *Am. J. Crit. Care* **18**, 319–328, quiz 329.
- Soares, R. B., W. Myakawa, R. S. Navarro, A. Baptista, M. S. Ribeiro and S. C. Nunez (2018) Photodynamic therapy to destroy pneumonia associated microorganisms using external irradiation source. In *Light-Based Diagnosis and Treatment of Infectious Diseases*, Proceedings of SPIE 10479, 1047917. San Francisco, California:SPIE.
- Bassi, G. L., M. Ferrer, J. D. Marti, T. Comaru and A. Torres (2014) Ventilator-associated pneumonia. *Semin. Respir. Crit. Care Med.* **35**, 469–481.
- Lee, C. F., C. J. Lee, C. T. Chen and C. T. Huang (2004) delta-Aminolaevulinic acid mediated photodynamic antimicrobial chemotherapy on *Pseudomonas aeruginosa* planktonic and biofilm cultures. *J. Photochem. Photobiol. B* **75**, 21–25.
- Tan, Y., Q. Cheng, H. Yang, H. Li, N. Gong, D. Liu, J. Wu and X. Lei (2018) Effects of ALA-PDT on biofilm structure, virulence factor secretion, and QS in *Pseudomonas aeruginosa*. *Photodiagnosis Photodyn. Ther.* **24**, 88–94.
- de Melo, W. C., P. Avci, M. N. de Oliveira, A. Gupta, D. Vecchio, M. Sadasivam, R. Chandran, Y. Y. Huang, R. Yin, L. R. Perussi, G. P. Tegos, J. R. Perussi, T. Dai and M. R. Hamblin (2013) Photodynamic inactivation of biofilm: taking a lightly colored approach to stubborn infection. *Expert Rev. Anti Infect. Ther.* **11**, 669–693.
- Diaconu, O., I. Siroopol, L. I. Poloşanu and I. Grigoraş (2018) Endotracheal tube biofilm and its impact on the pathogenesis of ventilator-associated pneumonia. *J. Crit. Care Med. (Targu Mures)* **4**, 50–55.
- Pneumatikos, I. A., C. K. Dragoumanis and D. E. Boursos (2009) Ventilator-associated pneumonia or endotracheal tube-associated pneumonia? An approach to the pathogenesis and preventive strategies emphasizing the importance of endotracheal tube. *Anesthesiology* **110**, 673–680.
- Metcalfe, D., C. Robinson, D. Devine and S. Wood (2006) Enhancement of erythrosine-mediated photodynamic therapy of *Streptococcus mutans* biofilms by light fractionation. *J. Antimicrob. Chemother.* **58**, 190–192.
- Misba, L. and A. U. Khan (2018) Enhanced photodynamic therapy using light fractionation against *Streptococcus mutans* biofilm: type I and type II mechanism. *Future Microbiol.* **13**, 437–454.
- Rouze, A., I. Martin-Loeches and S. Nseir (2018) Airway devices in ventilator-associated pneumonia pathogenesis and prevention. *Clin. Chest Med.* **39**, 775–783.
- Flemming, H. C. and J. Wingender (2010) The biofilm matrix. *Nat. Rev. Microbiol.* **8**, 623–633.
- Garcez, A. S., S. C. Nunez, N. Azambuja Jr, E. R. Fregnani, H. M. H. Rodriguez, M. R. Hamblin, H. Suzuki and M. S. Ribeiro (2013) Effects of photodynamic therapy on Gram-positive and Gram-negative bacterial biofilms by bioluminescence imaging and scanning electron microscopic analysis. *Photomed. Laser Surg.* **31**, 519–525.
- Suarez, C., M. Piculell, O. Modin, S. Langenheder, F. Persson and M. Hermansson (2019) Thickness determines microbial community structure and function in nitrifying biofilms via deterministic assembly. *Sci. Rep.* **9**, 5110.